

# POLARIZATION OF FLEXURAL WAVES IN AN ANISOTROPIC BOREHOLE MODEL

Zhenya Zhu, C. H. Cheng, and M. Nafi Toksöz

Earth Resources Laboratory  
Department of Earth, Atmospheric, and Planetary Sciences  
Massachusetts Institute of Technology  
Cambridge, MA 02139

## ABSTRACT

Two modes of flexural waves can be generated by a dipole source in an anisotropic borehole. Their velocities are related to those of the fast and slow shear waves in the formation. The particle motions and the polarization diagrams of the fast and slow flexural waves are measured in borehole models made of phenolite materials with transverse isotropy or orthorhombic anisotropy. The experimental results show that the particle motion of the fast flexural wave is linear and in the same direction as that of the fast shear wave in the formation. The polarization direction of the fast flexural wave coincides with that of the fast shear wave and is independent of the direction of the dipole source. The particle motion of the slow flexural wave is nonlinear and elliptic. Its polarization direction and variation are dependent on the anisotropic material and the source direction. This means that the slow flexural wave is a more complicated wave mode rather than the simple mode where the particle motion generated by a dipole source is in the direction of the slow shear wave. The polarization characteristics of the fast flexural wave can be applied to determine the principal axis of an anisotropic formation by in-line and cross-line logging data.

## INTRODUCTION

The rapid development of the dipole direct shear wave logging benefits from the fact that it can be applied not only in an open borehole, but also in a cased borehole surrounded by either a hard or a soft formation (Schmitt, 1989; Chen and Eriksen, 1991). It is a very useful means to explore the azimuthal anisotropy of a formation due to the polarization of dipole source and the receiver in the plane perpendicular to the borehole axis (Leslie and Randall, 1992).

The shear velocity in a certain direction of the anisotropic material depends on the direction of the particle vibration. In general, the shear wave splits into two waves propagating at different speeds and with particle vibrations perpendicular to each other (Alford, 1986; Cheadle *et al.*, 1991). The evaluation of anisotropy by shear wave splitting has potential application in the detection of fractures, cracks and other inclusions (Crampin, 1985; Lo *et al.*, 1986; Winterstein, 1987). The flexural wave generated by a dipole source in a fluid-filled borehole surrounded by an anisotropic formation also splits into fast and slow waves whose velocities are related to those of fast and slow shear waves (Esmersoy, 1990; Zhu *et al.*, 1993; Esmersoy *et al.*, 1994), respectively. The borehole wave particle motion in anisotropic formations has been observed and analyzed with data recorded in VSP surveys (Leary *et al.*, 1987; Barton and Zoback, 1988; Leveille and Seriff, 1989).

The polarization and the particle motion of the fast and slow flexural waves, as well as the relationship between the flexural and shear waves, are investigated with anisotropic borehole models in this paper. The experimental results show the different polarization diagrams of the fast and slow flexural waves and provide the evidence to explain the received flexural waveforms.

## FLEXURAL WAVES IN AN ISOTROPIC BOREHOLE

The measurements are conducted with an isotropic lucite borehole model to check the dipole transducers and the electronic system, and to compare the results with those in an anisotropic model. Figure 1 shows a diagram of the lucite model and the measuring system. The mono/dipole transducers are applied as source or receiver (Zhu *et al.*, 1993). The electric signal exciting the source transducer is a  $\delta$ -pulse. Received signals are amplified by a wide-band amplifier (20kHz-2MHz). Then they are recorded by a digital oscilloscope without any electronic filter. The recorded signals can be numerically filtered during data processing.

When the polarization of the dipole source is fixed in a certain direction and the spacing between the source and the receiver is constant, the dipole receiver is rotated and the received waveforms are recorded (Figure 2). Because the borehole and the dipole transducer are not exactly symmetric under experimental conditions, not only the flexural wave, but also the high-frequency P-wave are clearly recorded in Figure 2. Their amplitudes vary with the azimuth of the dipole receiver. The P-wave and flexural wave are completely separated in the time domain of the received waveforms. We measure their maximum amplitude at different azimuths and show the polarization in Figure 3, respectively. The arrow indicates the excitation direction of the dipole source. The main lobes in the polarization diagram are not exactly symmetric. Perhaps this is caused by two facts: the non-symmetry of the dipole source due to the limitations of the technology for making the transducer, and the source or receiver is not located exactly in the center of the borehole. Therefore, only part of the component propagating with P-wave velocity is received and recorded. The polarization of the P-wave indicates

## Flexural Waves in an Anisotropic Borehole Model

the direction of the dipole source.

Figure 3 shows that the polarization of the P-wave and the flexural wave in the lucite borehole model is in good agreement with the direction of the dipole source. The particle motions of the P-wave and flexural wave can be drawn with the recorded wave traces in Figure 2. Figure 4 draws the particle motions of the P-wave (Figure 4a) and the flexural wave (Figure 4b), which are picked up from two traces perpendicular to each other. From Figure 4 it can be seen that the particle motions of both the P-wave and the flexural wave are almost linear and their direction is in the same direction of the dipole source.

## FLEXURAL WAVES IN AN ANISOTROPIC BOREHOLE

The acoustic fields, both axial and azimuthal, generated by a dipole source are measured in the borehole models made of anisotropic man-made materials. First we introduce the acoustic property of the materials and then show the waveforms recorded in our experiments.

### Acoustic Anisotropy of the Modeling Materials

Two kinds of anisotropic phenolite materials are selected in our experiments—(1) phenolite XX-324 with transverse isotropy, and (2) phenolite CE-578 with orthorhombic anisotropy. These materials are composed of laminated sheets of paper or canvas fabric. The sizes of the phenolite blocks are  $25.4 \times 25.4 \times 5.1\text{cm}^3$  and  $25.4 \times 25.4 \times 17.8\text{cm}^3$ , respectively. The P- and S-velocities along the principal axes of the blocks are measured with P- and S-wave transducers, respectively. Figure 5 shows the velocity distribution along the three axes.

Because the two velocities of the shear waves propagating along the Z-axis of the phenolite XX-324 block have the same speed, the material is transversely isotropic, but the P-wave velocities along the X-axis and the Y-axis are different. If a borehole is drilled along the X-axis or the Y-axis, it is an azimuthally anisotropic borehole model. From Figure 5a, we see that the fast shear velocity here is faster than that in water and the slow one is slower than that in water. The anisotropy of the shear wave is about 28%.

The anisotropy of phenolite CE-578 is less than that of phenolite XX-324 (Cheadle *et al.*, 1991). The anisotropies of phenolite CE-578 along the X axis and the Y axis are 9.3% and 3.7%, respectively. All of the shear velocities are very close to the velocity in water.

Three holes with 1.27 cm in diameter are drilled along the X-axis of the phenolite XX-324, the X-axis, and the Y-axis of the phenolite CE-578, respectively. To eliminate the boundary influence of the phenolite XX-324 block at the Z-axis, two similar blocks are glued firmly to the drilled block to form a borehole model with a size of  $25.4 \times 25.4 \times 15.3\text{cm}^3$ .

## Axial Acoustic Field in an Anisotropic Borehole

To distinguish acoustic waves generated in the three anisotropic borehole models, array measurements are performed with monopole and dipole transducers in a water tank. The received waveforms are recorded, while the source transducer is fixed at a certain location in the boreholes and the receiver is moved step-by-step along the borehole axis. The borehole models are shown in Figure 6. The measuring system is the same one as that in Figure 1. Because the frequency bands of the electronic source signal ( $\delta$ -pulse), the preamplifier, and the oscilloscope are wider than that of received acoustic waves, the frequency band of the received waveforms mainly depends on the borehole excitation, the frequency dispersions of the acoustic modes, and the frequency response of the source and receiver.

Figures 7–9 show the array waveforms received with a monopole and a dipole system in the three borehole models, respectively. There are P-waves, S-waves, pseudo-Rayleigh waves, and Stoneley waves in the seismograms generated by the monopole. From the seismograms generated by the dipole transducer, we can see that there are high-frequency components propagating with P-wave velocity and both fast and slow flexural waves distinguished by their different velocities. The fast flexural wave is of high frequency and low amplitude; particularly its amplitude is very small in the phenolite CE-578 model. On the other hand, the slow flexural wave is of low frequency and high amplitude. We have discussed and compared the difference between the slow flexural wave and the Stoneley wave (Zhu *et al.*, 1993). They are different acoustic modes distinguished by their propagating velocity and amplitude variation in azimuths.

## Radial Acoustic Field in an Anisotropic Borehole

Two kinds of flexural waves—fast and slow ones—in an azimuthally anisotropic borehole have been confirmed by the above array measurements. To investigate the polarization of the fast and slow flexural waves in an anisotropic borehole, we measure the azimuthal acoustic field generated by a dipole source. While the dipole source is fixed at a certain azimuth and the spacing between the dipole source and the receiver is also fixed, the receiver is rotated step-by-step in the borehole and the received signals are digitally recorded.

Figures 10–12 show the typical seismograms recorded in the phenolite XX-324 model, the phenolite CE-578 model with an X-direction borehole, and that with a Y-direction borehole, while the polarization direction of the dipole source is located at  $30^\circ$ , respectively. In each plot, 40 traces are recorded with the dipole receiver rotating clockwise with an azimuth increase of  $9.72^\circ$ /trace starting from  $0^\circ$ . The  $0^\circ$ -direction is that of the fast shear wave in the anisotropic models. A total of 21 plots is recorded when the dipole source is located at  $0^\circ, 30^\circ, 60^\circ, 90^\circ, 120^\circ, 150^\circ$ , and  $180^\circ$  in the three models. Only three of the plots are shown here. From these waveforms we can further investigate the variations of the amplitudes of the fast and slow flexural waves with the azimuths.

## Flexural Waves in an Anisotropic Borehole Model

### POLARIZATION OF THE FLEXURAL WAVES IN AN ANISOTROPIC BOREHOLE

The particle motion diagrams and the polarization of the acoustic waves with different modes are studied by means of waveforms recorded in the above measurements.

#### Flexural Waves in the Borehole of Phenolite XX-324

Both the particle motion and the polarization of the flexural waves in a phenolite XX-324 borehole model are studied.

#### Particle Motion

The fast and slow flexural waves can be selected from the waveforms recorded at two locations where the directions of the receiver are perpendicular to each other. The particle motion diagrams can be drawn with the amplitude of the selected waves. Figures 13-16 show the particle motions of the P-wave, and the fast and slow flexural waves, respectively. The arrows in these figures indicate the direction of the dipole source except in Figure 15 where the arrows indicate the direction of the fast shear wave.

Because the compressional wave propagating along the borehole axis is unique, the amplitude of its particle motion is only related to the direction of the dipole source. When the polarization of the dipole receiver is in the same direction as that of the source, the maximum P-wave amplitude should be recorded. Thus the real direction of the dipole source can be determined by the P-wave particle motion. Figure 13 shows that the actual source direction determined from the P-wave particle motion is in good agreement with that indicated by the arrow.

Figure 14 shows the particle motion of the fast flexural wave. Although the direction of the dipole source indicated by the arrow varies, the direction of the particle motion is rarely changes and is always in the direction of the fast shear wave. However, from these particle motions we see that the particle motion is not exactly in the same direction as the fast shear wave. A possible reason is that the vibration direction of the fast flexural wave is not in the same direction as the geometric principal axis of the model. The angle difference between them may be around  $20^\circ$ . If this is true, the fast flexural wave should not be generated, or its amplitude should be at a minimum where the direction of the dipole source is perpendicular to that of the fast shear wave.

Figure 15 shows the particle motion drawn by means of two fast flexural waveforms which are selected from the traces where the polarizations of the dipole source and the receiver are in in-line or are perpendicular to each other (cross-line). In Figure 15 the arrow indicates the direction of the fast shear wave (Y-axis). From these plots we know that the direction of the particle motion of the fast flexural wave is almost in agreement with that of the fast shear wave (Y-axis direction). The real dipole logging tool applied in oil fields usually has two sets of dipole receivers perpendicular to each other. If the fast flexural waves are selected from the waveforms received by the two receivers,

similar particle motion can be obtained and the direction of the fast shear wave can be determined by that of the particle motion.

There is some difference between the directions of the particle motion and the fast shear wave. If the actual axis of the fast shear wave drifts off the geometric principal axis about  $20^\circ$ , the resulting particle motion in the direction of the fast shear wave would be better.

Figure 16 shows the particle motion of the slow flexural wave, which is a non-linear or elliptic motion. The direction of the elliptic axis varies with that of the dipole source.

### Polarization of the Flexural Waves

The polarization diagrams of the fast and the slow flexural waves can be drawn in a polar coordinate plot by the maximum amplitudes of the waves selected from the waveforms which are similar to those in Figure 10. Figure 17 shows the polarization diagrams of the fast and slow flexural waves in the phenolite XX-324 model when the dipole source is located at  $0^\circ$ ,  $30^\circ$ ,  $60^\circ$ ,  $90^\circ$ ,  $120^\circ$ ,  $150^\circ$ , and  $180^\circ$ , respectively. The arrow indicates the direction of the dipole source. The polarization diagrams are very similar to the radiation pattern of the dipole source. There is an apparent direction where the received amplitude is maximum. The polarization of the fast flexural wave is almost fixed in the  $0^\circ$ -direction (the direction of the fast shear wave or Y-axis). In contrast, the polarization of the slow flexural wave varies with the direction of the dipole source. When the polarization of the source rotates counterclockwise from  $0^\circ$  (Y-axis) to  $180^\circ$ , the polarization of the slow flexural wave rotates counterclockwise from  $-30^\circ$  to  $150^\circ$  approximately. The angle between them is about  $30^\circ$  and does not vary with the direction of the dipole source. This means that the fast and the slow flexural waves have different characteristics. The fast one is closely related to the fast shear wave in the anisotropic formation. The slow one is a more complicated wave than the fast one. It is related not only to the slow shear wave, but also to the polarization of the dipole source.

### Flexural Waves in the Borehole of Phenolite CE-578

Figures 18–19 show the polarization of the slow flexural waves generated by a dipole source at various azimuths in the X-axis and the Y-axis borehole models of phenolite CE-578, respectively. We see that the polarization of the slow flexural wave varies with the direction of the dipole source and the regular pattern of the variation is different from that in the borehole of phenolite XX-324. When the direction of the source varies counterclockwise from  $0^\circ$  to  $180^\circ$  in Figure 18, the polarization of the slow flexural wave varies clockwise from  $60^\circ$  to  $240^\circ$ . The same regularity of the variation can be seen in Figure 19, but it is not very clear.

## Flexural Waves in an Anisotropic Borehole Model

### CONCLUSIONS AND DISCUSSION

Our experimental results show that two modes of the flexural wave can be generated by a dipole source in an azimuthally anisotropic borehole. The flexural wave at higher frequency with faster velocity is called a fast flexural wave. The second one is called a slow flexural wave. Their velocities are close to, but slower than, those of the fast and the slow shear waves in the anisotropic formation, respectively. The excitation of the fast flexural wave is related to the formation surrounding the borehole. The amplitude of the fast flexural wave generated in the borehole of phenolite CE-578 is much smaller than that of phenolite XX-324.

In the isotropic lucite borehole model, the particle motion of the flexural wave is linear and its polarization varies completely with the direction of the dipole source.

The polarization and the particle motion direction of the fast flexural wave in an anisotropic borehole are almost in the same direction of the fast shear wave in the formation and do not vary with the direction of the dipole source. When the direction of the dipole source is perpendicular to that of the fast shear wave, hardly any fast flexural wave is generated. According to this characteristic of the fast flexural wave, the principal axis of the fast shear wave can be determined by its particle motion from waveforms received with in-line and cross-line dipole receivers.

The locus of the particle motion of the slow flexural wave is non-linear. The direction of the polarization varies with that of the dipole source and is related to the anisotropy of the formation. Therefore, the slow flexural wave in an anisotropic borehole is a complicated wave contributed by the waves whose particle motions are in the directions of both the fast and the slow shear waves.

### ACKNOWLEDGMENTS

This study is supported by the Borehole Acoustics and Logging Consortium at M.I.T., and Department of Energy contract no. DE-FG02-86ER13636.

REFERENCES

- Alford, R.M., 1986, Shear data in the presence of azimuthal anisotropy, *SEG 56th Ann. Internat. Mtg., Expanded Abstracts*, 476-479.
- Barton, C., and M. Zoback, 1988, Determination of in-situ stress orientation from borehole guided waves, *J. Geophys. Res.*, *93*, 7834-7844.
- Cheadle, S.P., R.J. Broun, and D.C. Lawton, 1991, Orthorhombic anisotropy: A physical seismic modeling study, *Geophysics*, *56*, 1603-1613.
- Chen, S.T., and A. Eriksen, 1991, Compressional and shear-wave logging in open and cased holes using a multipole tool, *Geophysics*, *56*, 550-557.
- Crampin, S., 1985, Evaluation of anisotropy by shear wave splitting, *Geophysics*, *50*, 142-152.
- Esmersoy, C., 1990, Split shear-wave inversion for fracture evaluation, *SEG 60th Ann. Internat. Mtg., Expanded Abstracts*, 1400-1403.
- Esmersoy, C., K. Koster, M. Williams, A. Boyd, and M. Kane, 1994, Dipole shear anisotropy logging, *SEG 64th Ann. Internat. Mtg., Expanded Abstracts*, 1139-1142.
- Leary, P.C., Y.G. Li, and K. Aki, 1987, Observation and modeling of fault-zone fracture seismic anisotropy, P, SV and SH traveltimes, *Geophys. J. Roy. Astr. Soc.*, *91*, 461-484.
- Leslie, H.D., and C.J. Randall, 1992, Multipole sources in deviated borehole penetrating anisotropic formations: Numerical and experimental results, *J. Acoust. Soc. Am.*, *91*, 12-27.
- Leveille, J.P., and A.J. Seriff, 1989, Borehole wave particle motion in anisotropic formations, *J. Geophys. Res.*, *94*, 7183-7188.
- Lo, T.W., K.B. Coyner, and M.N. Toksöz, 1986, Experimental determination of elastic anisotropy of Berea sandstone, Chicopee shale and Chelmsford granite, *Geophysics*, *51*, 164-171.
- Schmitt, D.P., 1989, Acoustic multipole logging in transversely isotropic poroelastic formations *J. Acoust. Soc. Am.*, *86*, 2397-2421.
- Winterstein, D.R., 1987, Shear waves in exploration: A perspective, *SEG 57th Ann. Internat. Mtg., Expanded Abstracts*, 638-641.
- Zhu, Z.Y., C.H. Cheng, and M.N. Toksöz, 1993, Propagation of flexural waves in an azimuthally anisotropic borehole model, *SEG 63rd Ann. Internat. Mtg., Expanded Abstracts*, 68-71.

# Flexural Waves in an Anisotropic Borehole Model

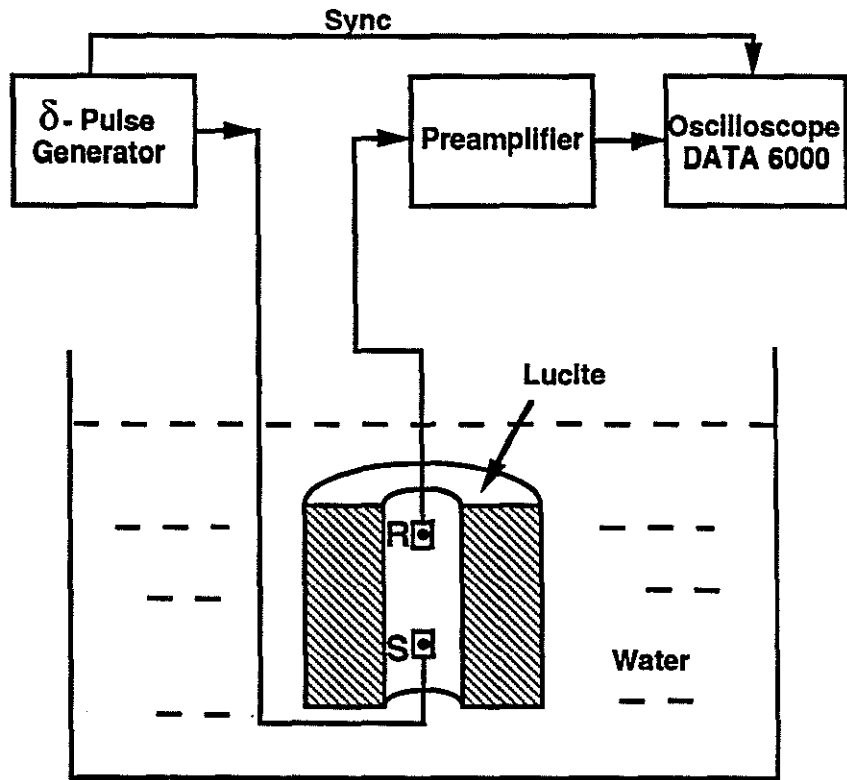


Figure 1: A lucite borehole model and diagrams of the measuring system.

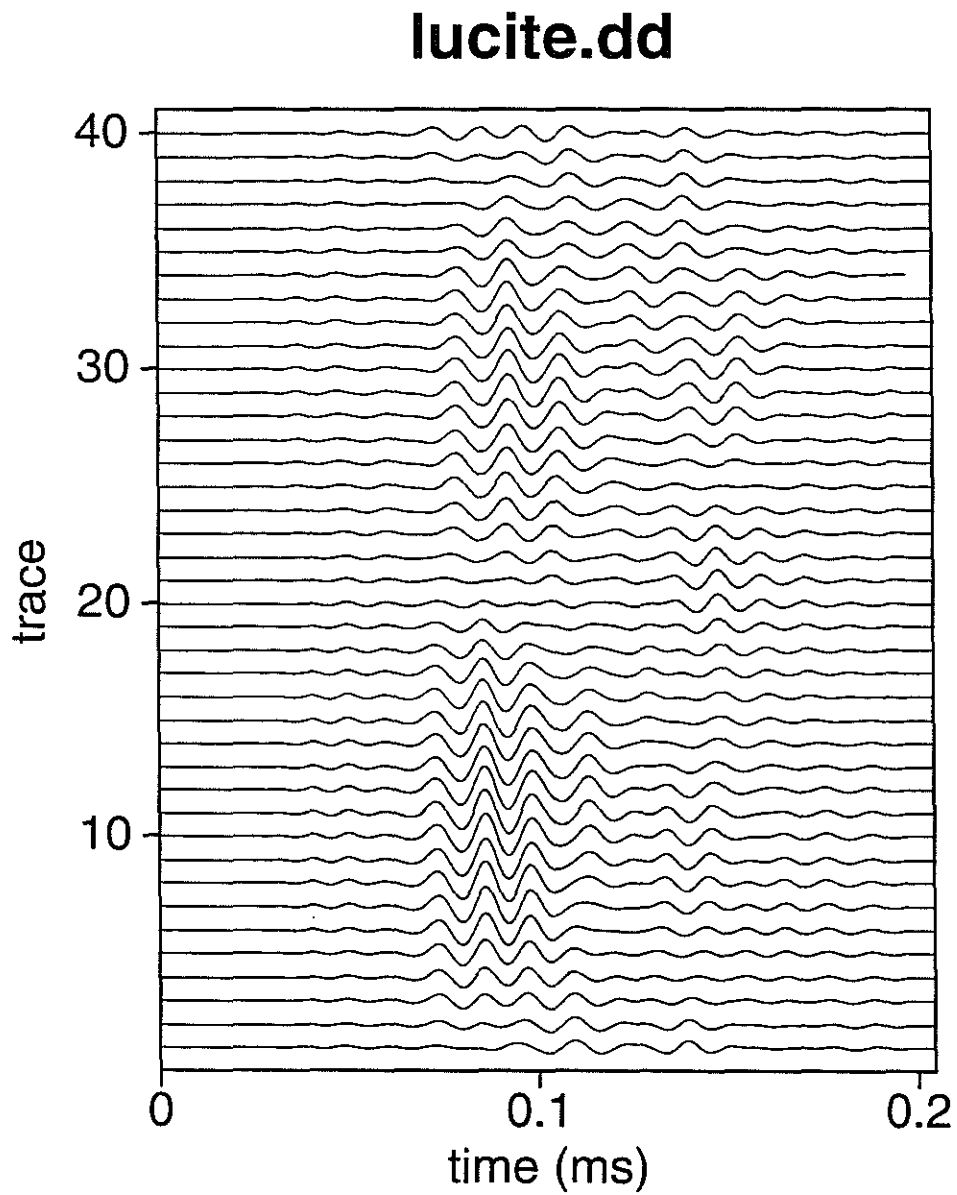


Figure 2: Waveforms recorded in the lucite borehole model by fixing the dipole source and rotating the dipole receiver with  $9.72^\circ/\text{trace}$ .

### Flexural Waves in an Anisotropic Borehole Model

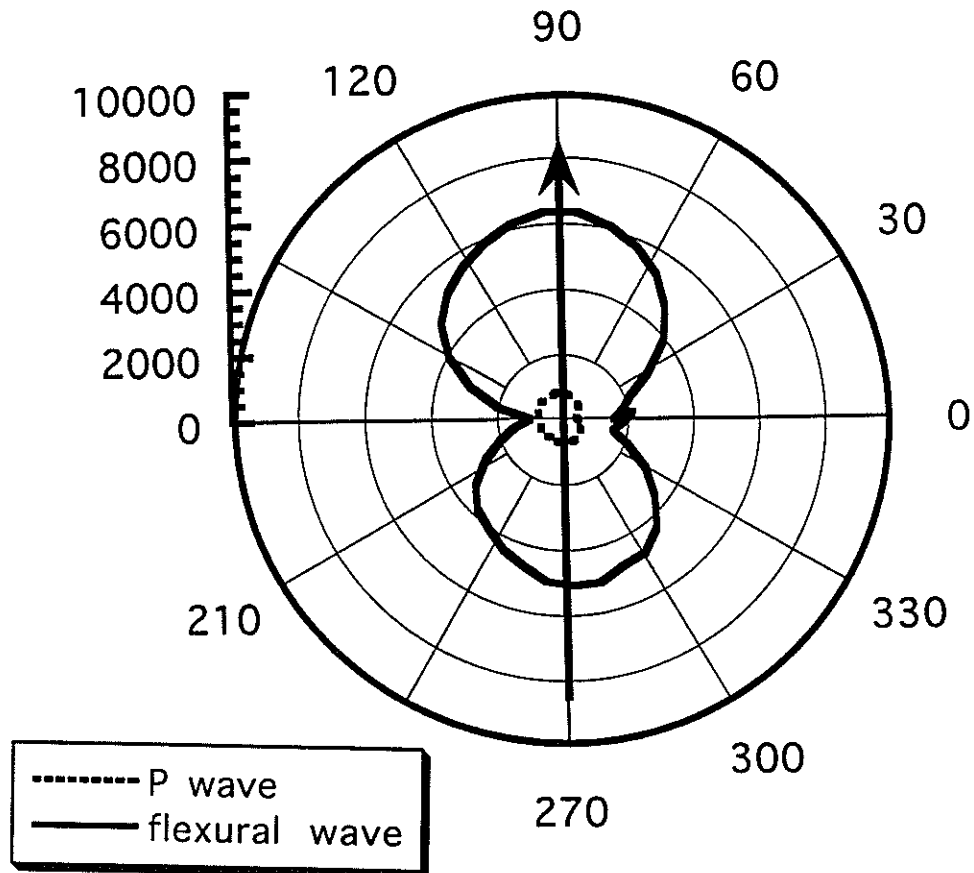


Figure 3: The polarizations of the P-wave (dash line) and the flexural wave (solid line) in the lucite model. The arrow indicates the direction of the dipole source.

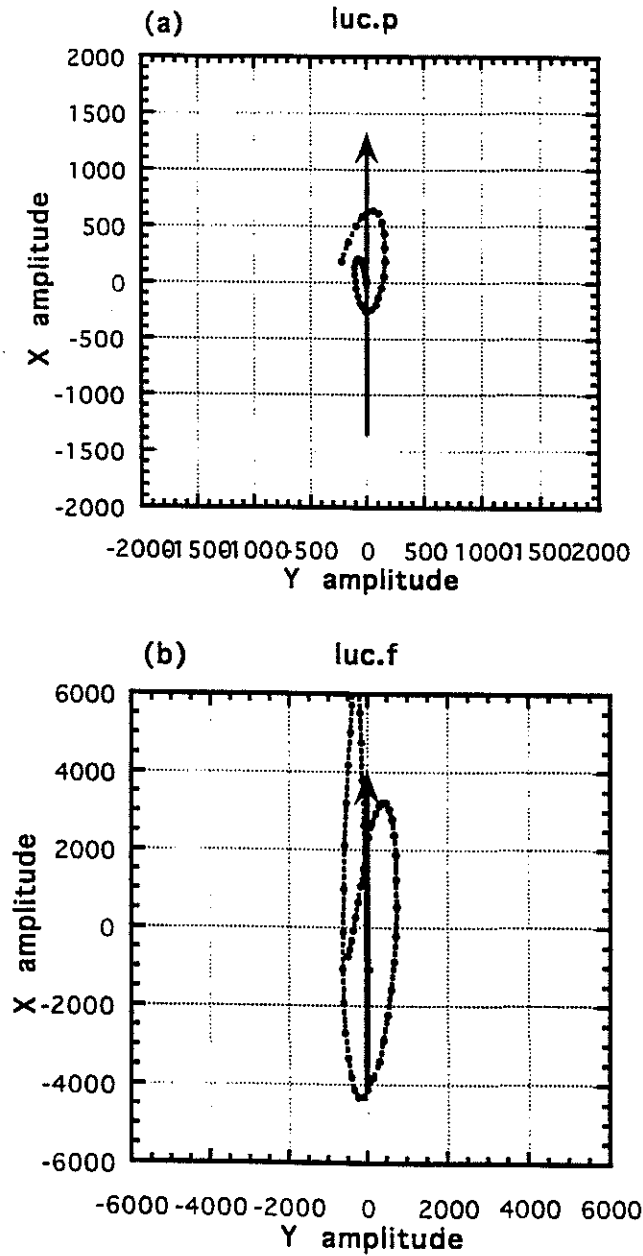
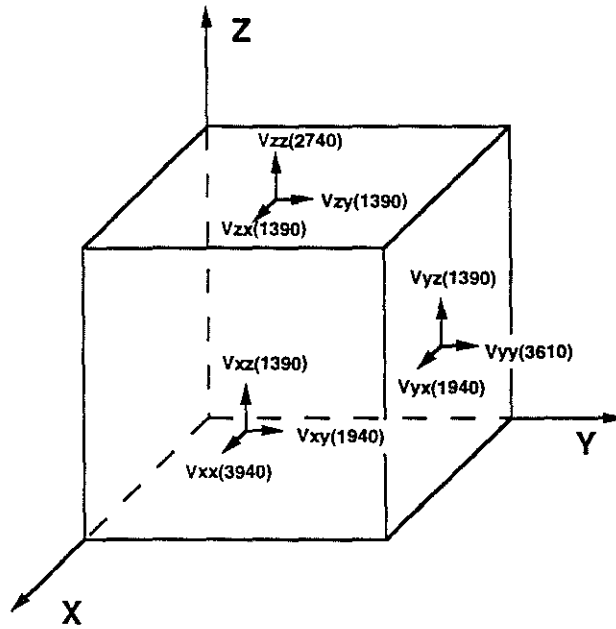
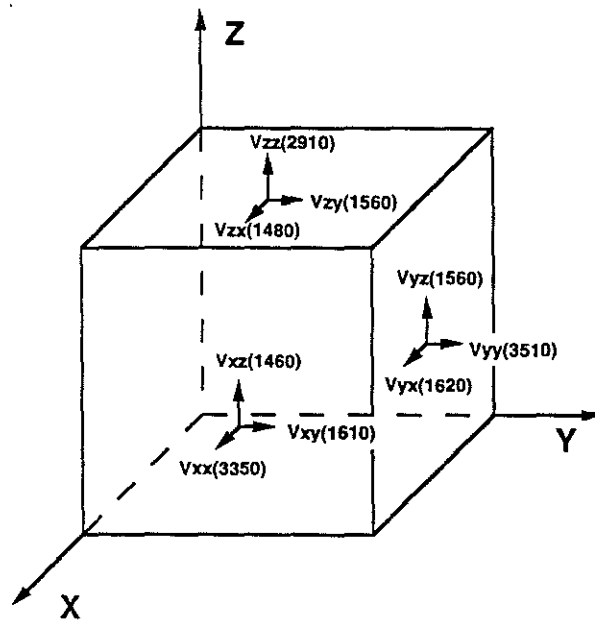


Figure 4: Particle motions of (a) P-wave and (b) flexural wave in a lucite model. The arrow indicates the direction of the dipole source.

# Flexural Waves in an Anisotropic Borehole Model

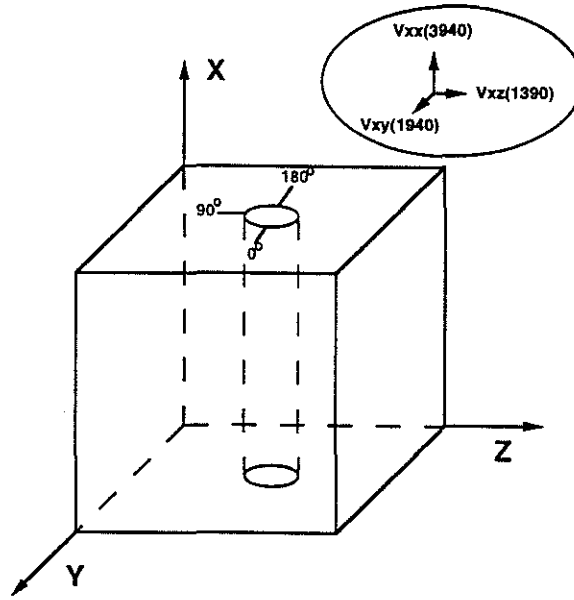


(a) Phenolite XX-324 (m/s)

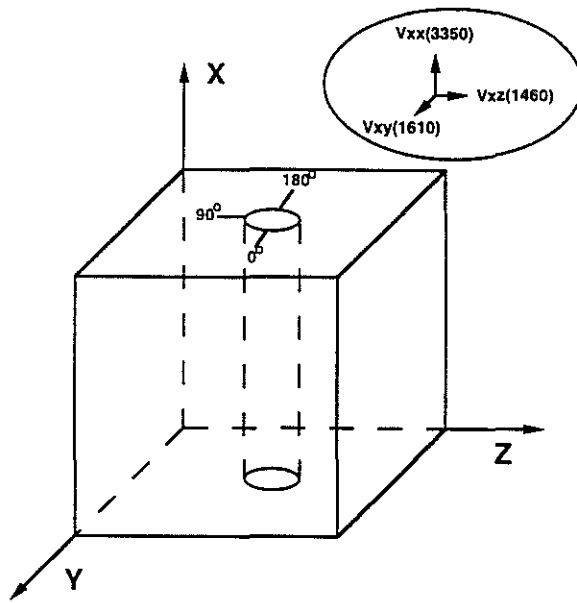


(b) Phenolite CE-578 (m/s)

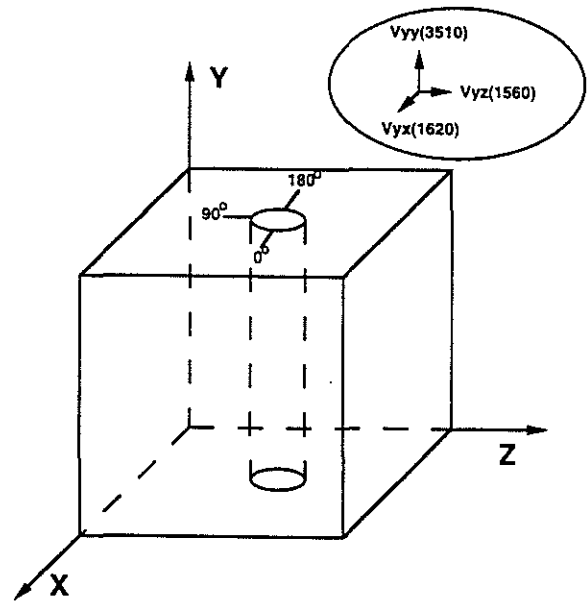
Figure 5: Velocity distribution (m/s) in (a) phenolite XX-324 and (b) phenolite CE-578.



(a) Phenolite XX-324



(b) Phenolite CE-578



(c) Phenolite CE-578

Figure 6: The anisotropic borehole models at X-axis of (a) phenolite XX-324, (b) X-axis of phenolite CE-578, and (c) Y-axis of phenolite CE-578.

## Flexural Waves in an Anisotropic Borehole Model

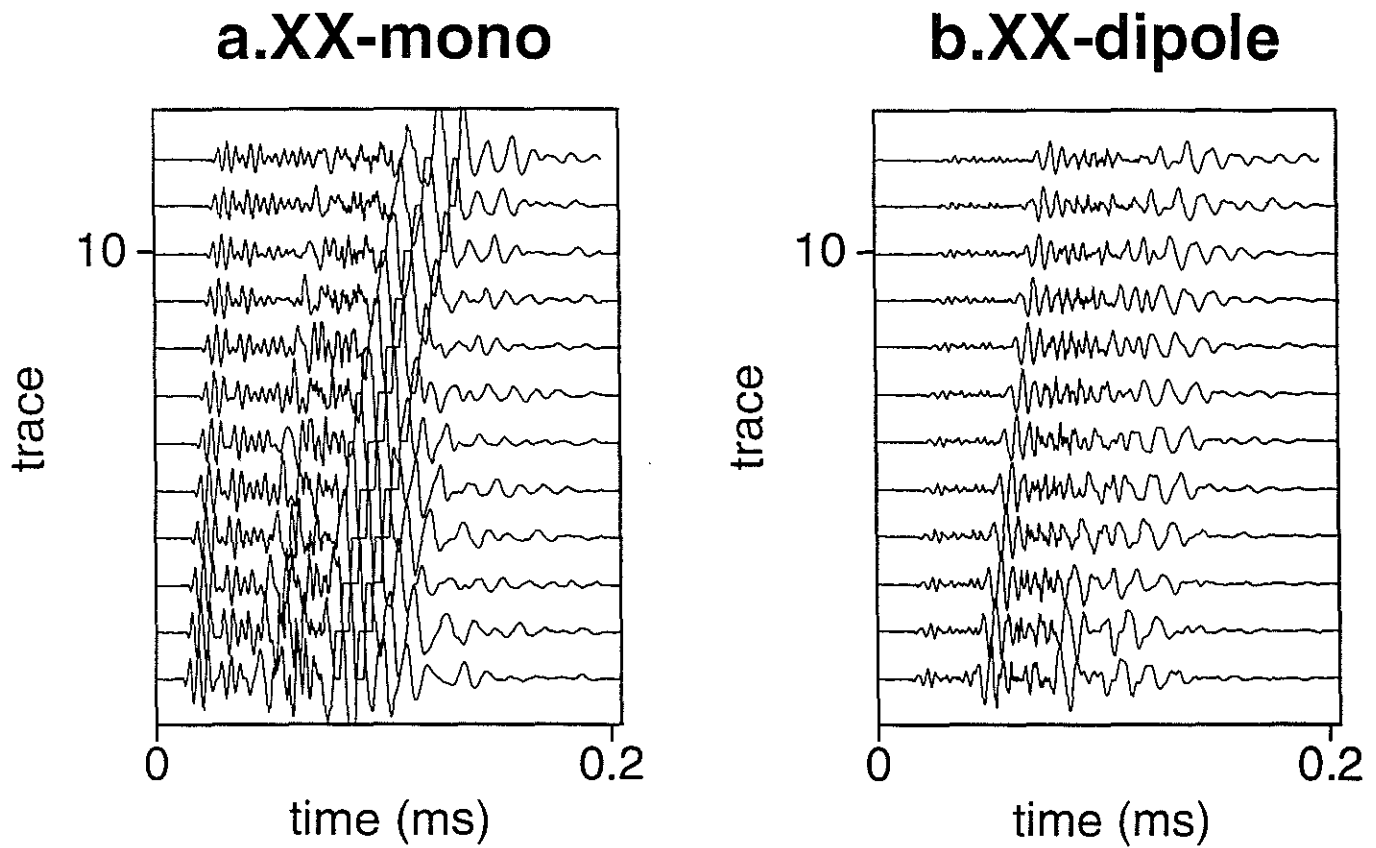


Figure 7: Waveforms recorded by (a) monopole transducers and (b) dipole transducers in the borehole model of phenolite XX-324. The spacing is 0.5 cm/trace.

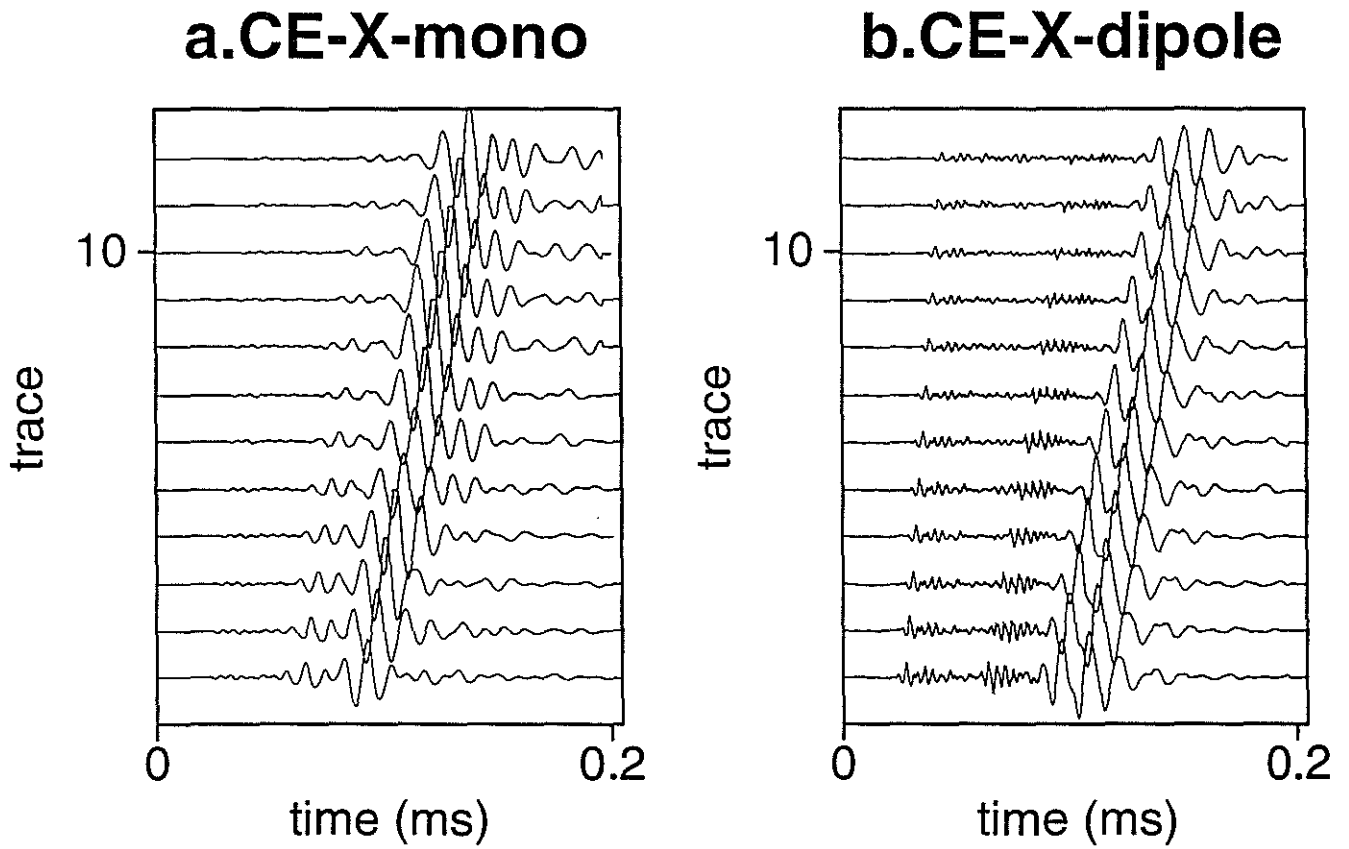


Figure 8: Waveforms recorded by (a) monopole transducers and (b) dipole transducers in the borehole model at X-axis of phenolite CE-578. The spacing is 0.5 cm/trace.

## Flexural Waves in an Anisotropic Borehole Model

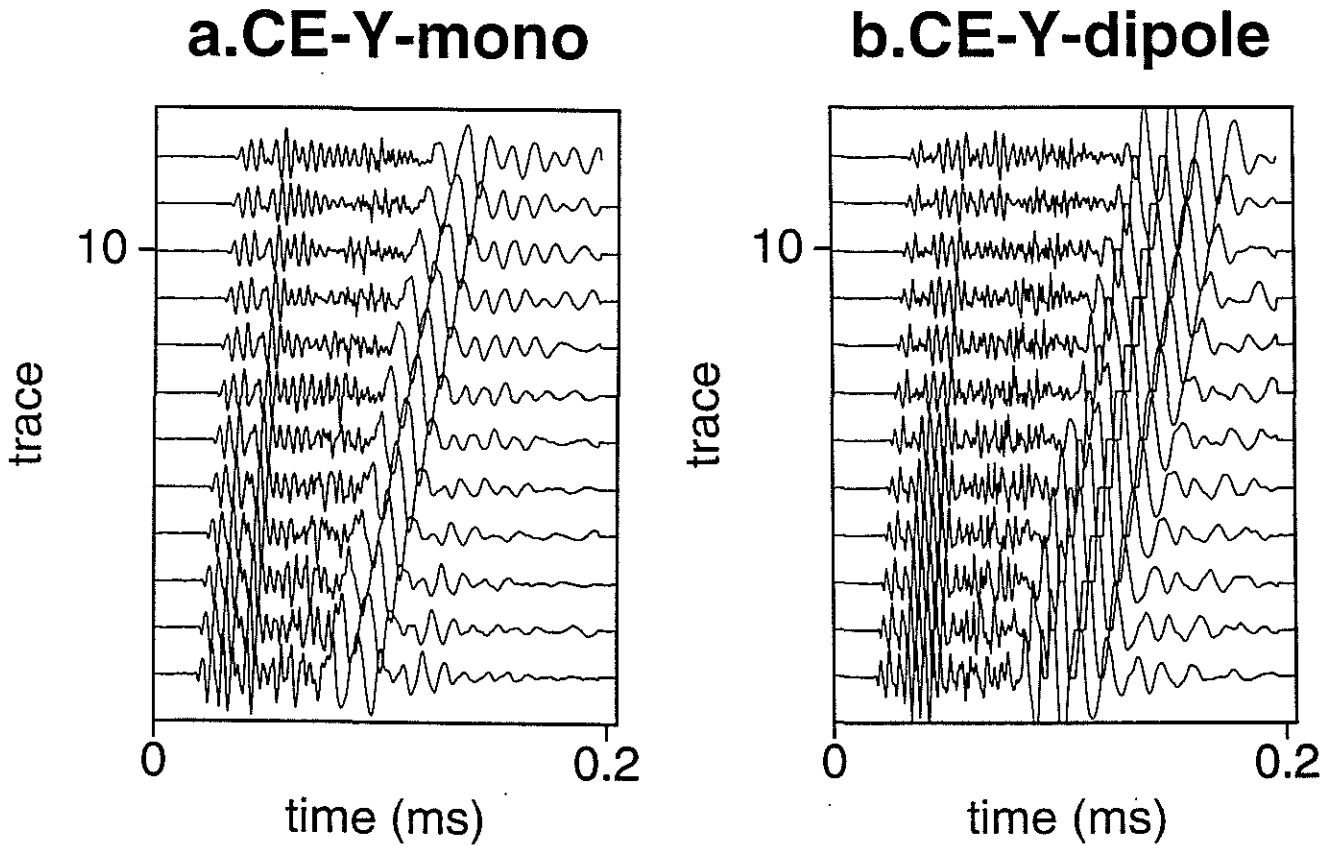


Figure 9: Waveforms recorded by (a) monopole transducers and (b) dipole transducers in the borehole model at Y-axis of phenolite CE-578. The spacing is 0.5 cm/trace.

## XX-30

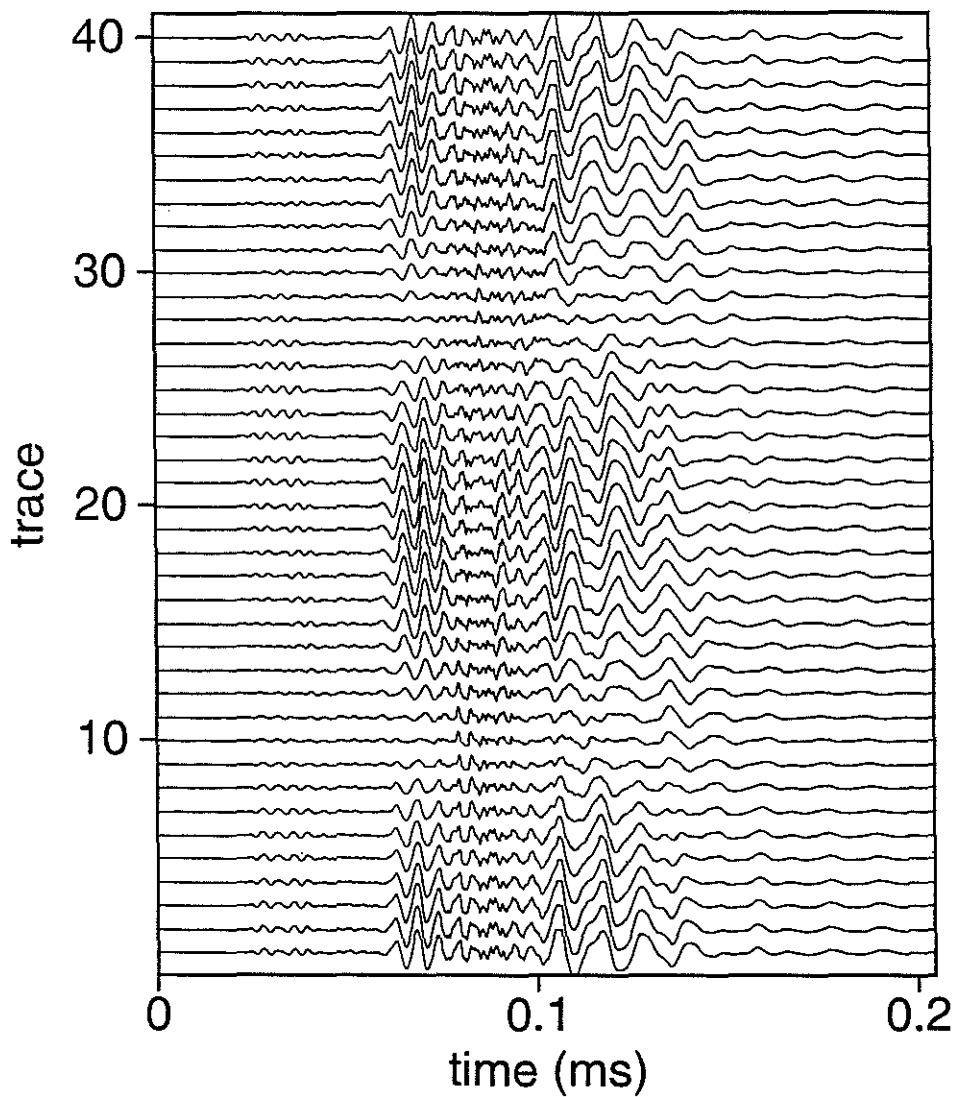


Figure 10: Waveforms recorded in the borehole of phenolite XX-324 by fixing the dipole source at  $30^\circ$  and rotating the dipole receiver with azimuth increasement of  $9.72^\circ$ /trace starting from the axis of the fast shear wave ( $0^\circ$  or Y-axis in Fig. 6).

Flexural Waves in an Anisotropic Borehole Model

**CE-X-30**

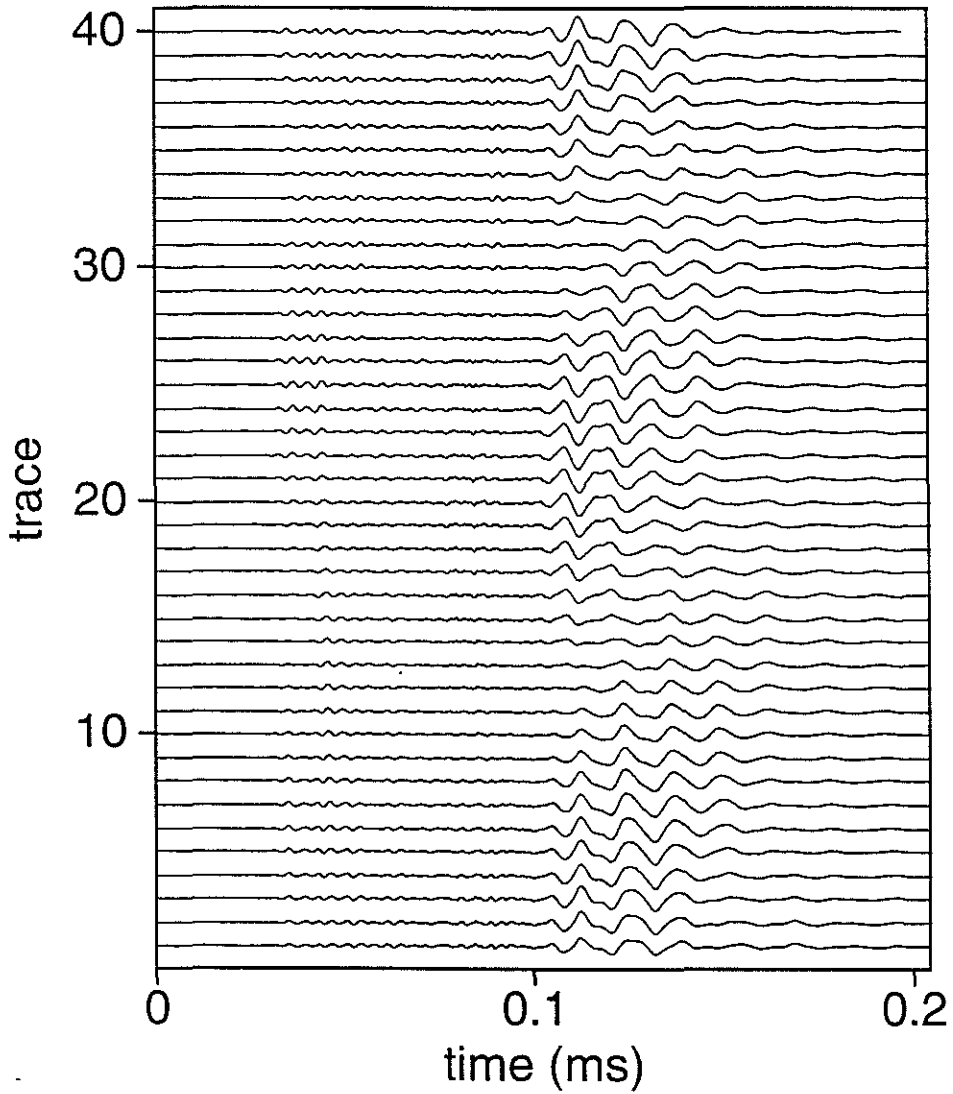


Figure 11: Waveforms recorded in the borehole at X-axis of phenolite CE-578 by fixing the dipole source at  $30^\circ$  and rotating the dipole receiver with azimuth increment of  $9.72^\circ$ /trace starting from the axis of the fast shear wave ( $0^\circ$  or Y-axis in Fig. 6).

## CE-Y-30

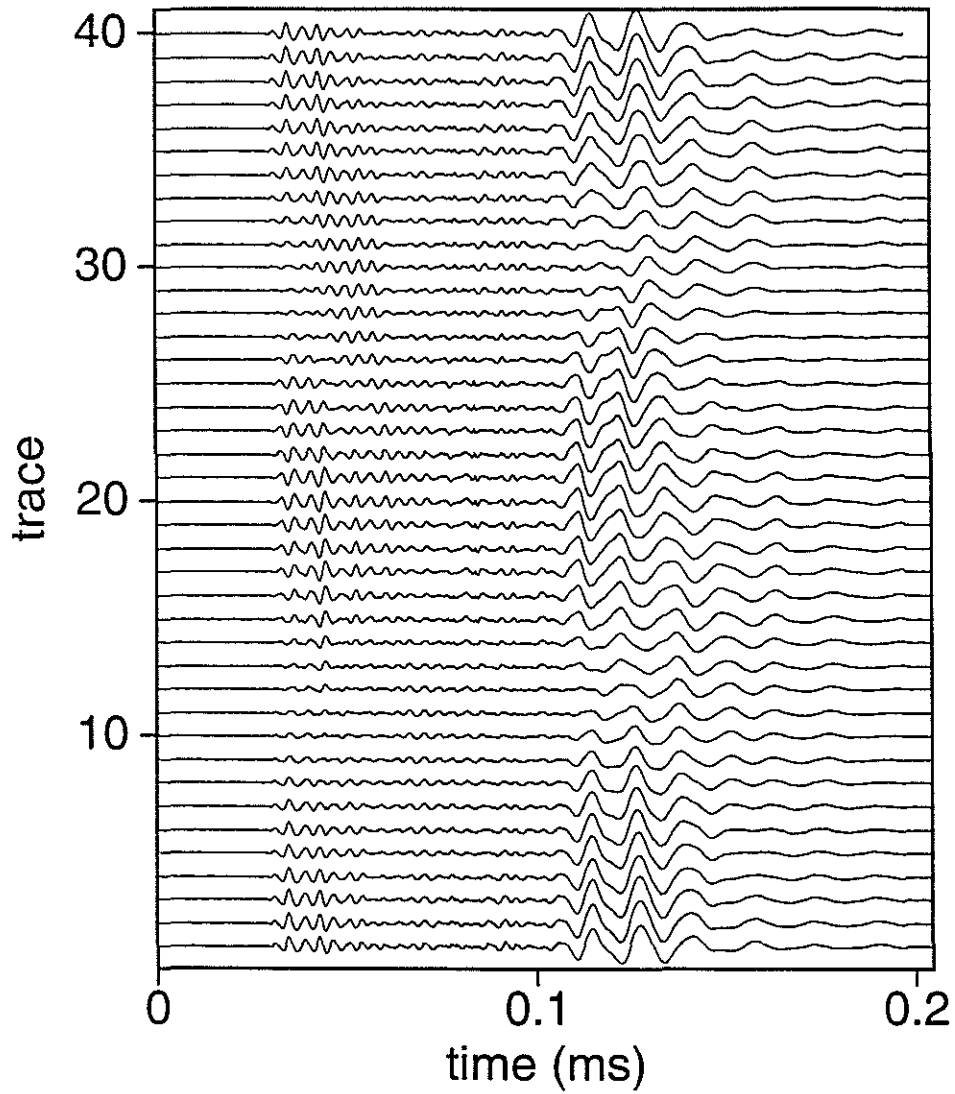


Figure 12: Waveforms recorded in the borehole at Y-axis of phenolite CE-578 by fixing the dipole source at  $30^\circ$  and rotating the dipole receiver with azimuth increasement of  $9.72^\circ$ /trace starting from the axis of the fast shear wave ( $0^\circ$  or X-axis in Fig 6).

## Flexural Waves in an Anisotropic Borehole Model

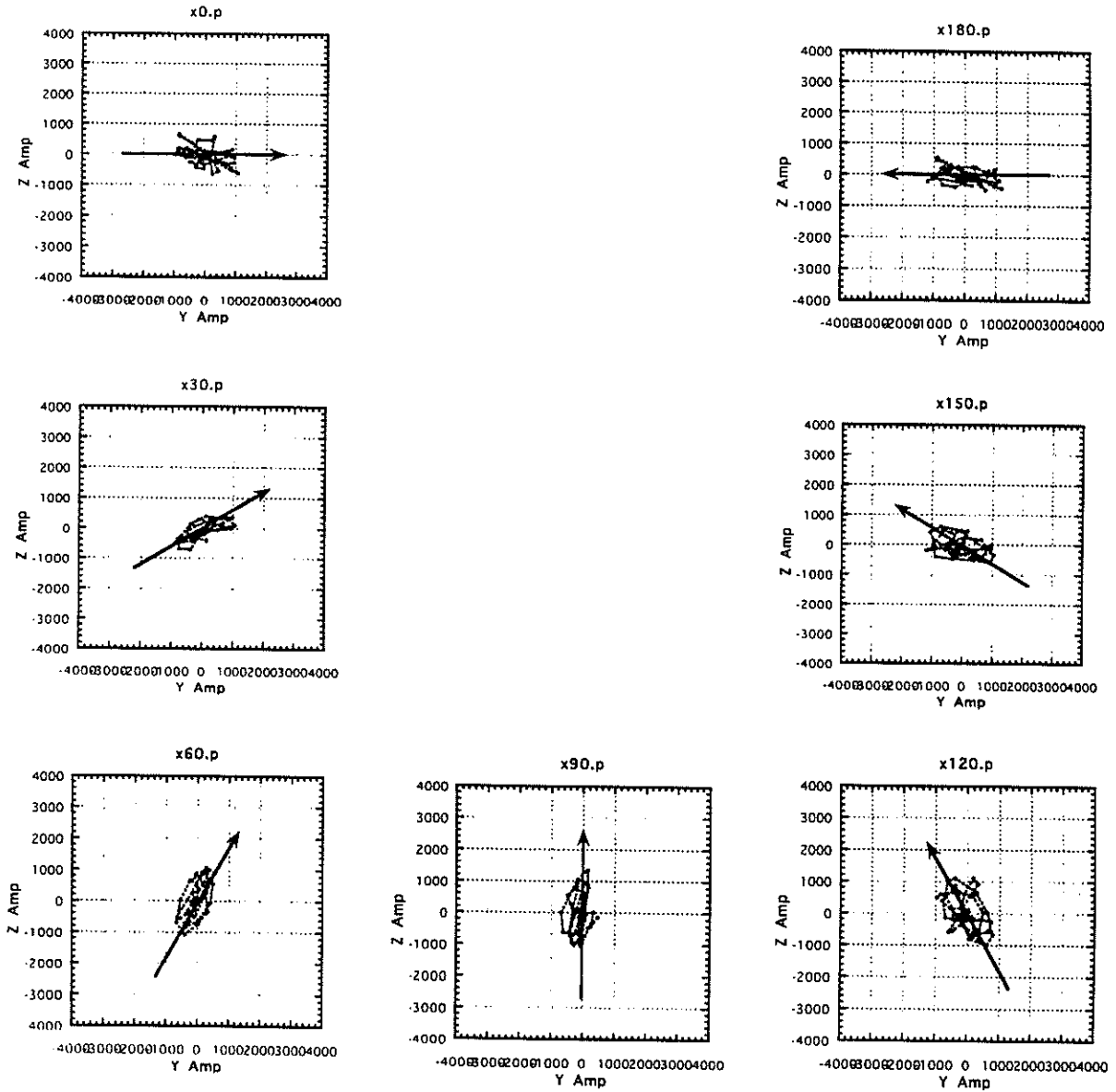


Figure 13: Particle motion of the P-wave components in the borehole of the phenolite XX-324. The arrow indicates the direction of the dipole source which is located at  $0^\circ$ ,  $30^\circ$ ,  $60^\circ$ ,  $90^\circ$ ,  $120^\circ$ ,  $150^\circ$ , and  $180^\circ$ , respectively.

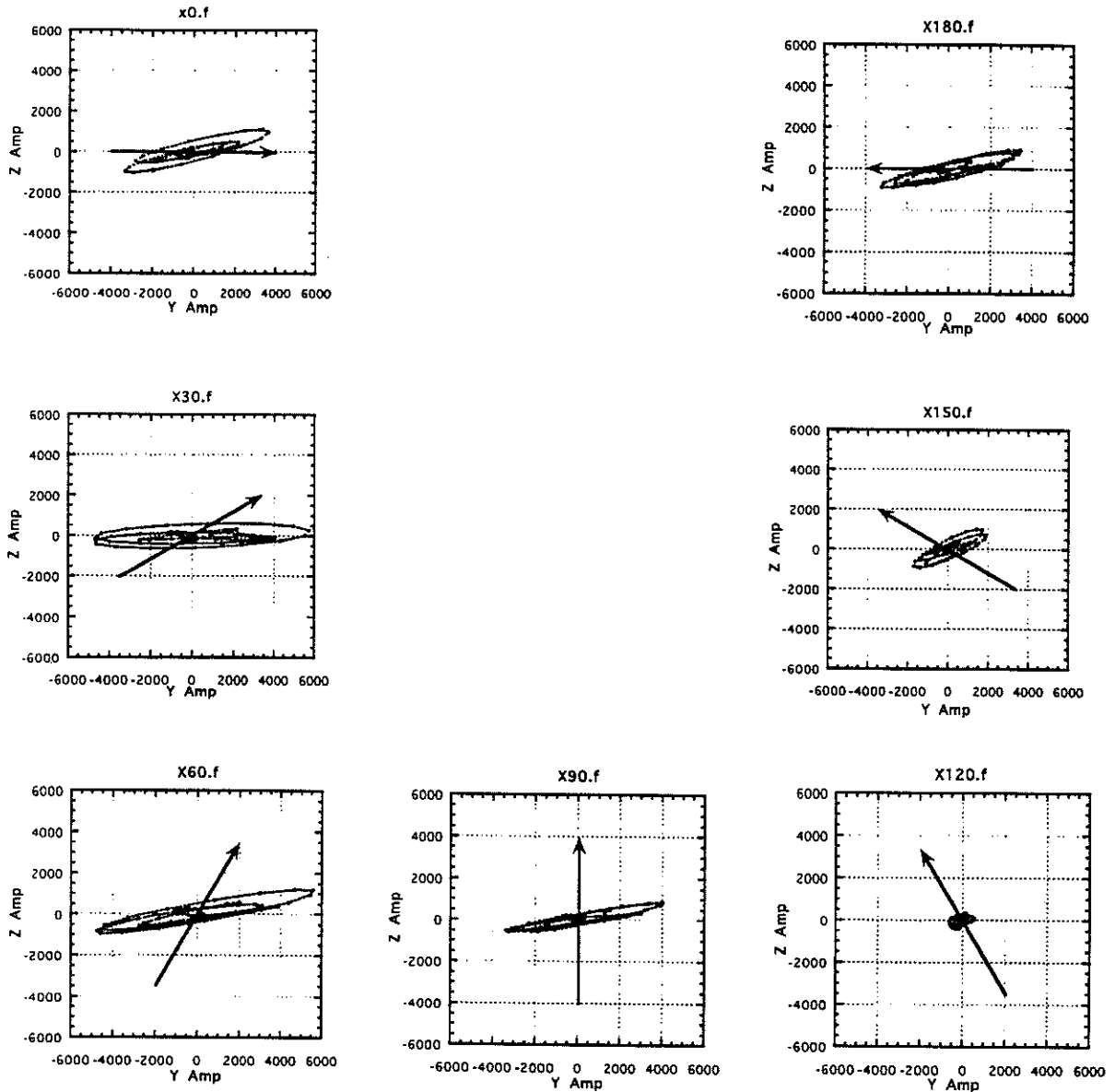


Figure 14: The particle motion of the fast flexural wave in the borehole of the phenolite XX-324. The arrow indicates the direction of the dipole source which is located at  $0^\circ$ ,  $30^\circ$ ,  $60^\circ$ ,  $90^\circ$ ,  $120^\circ$ ,  $150^\circ$ , and  $180^\circ$ , respectively.

## Flexural Waves in an Anisotropic Borehole Model

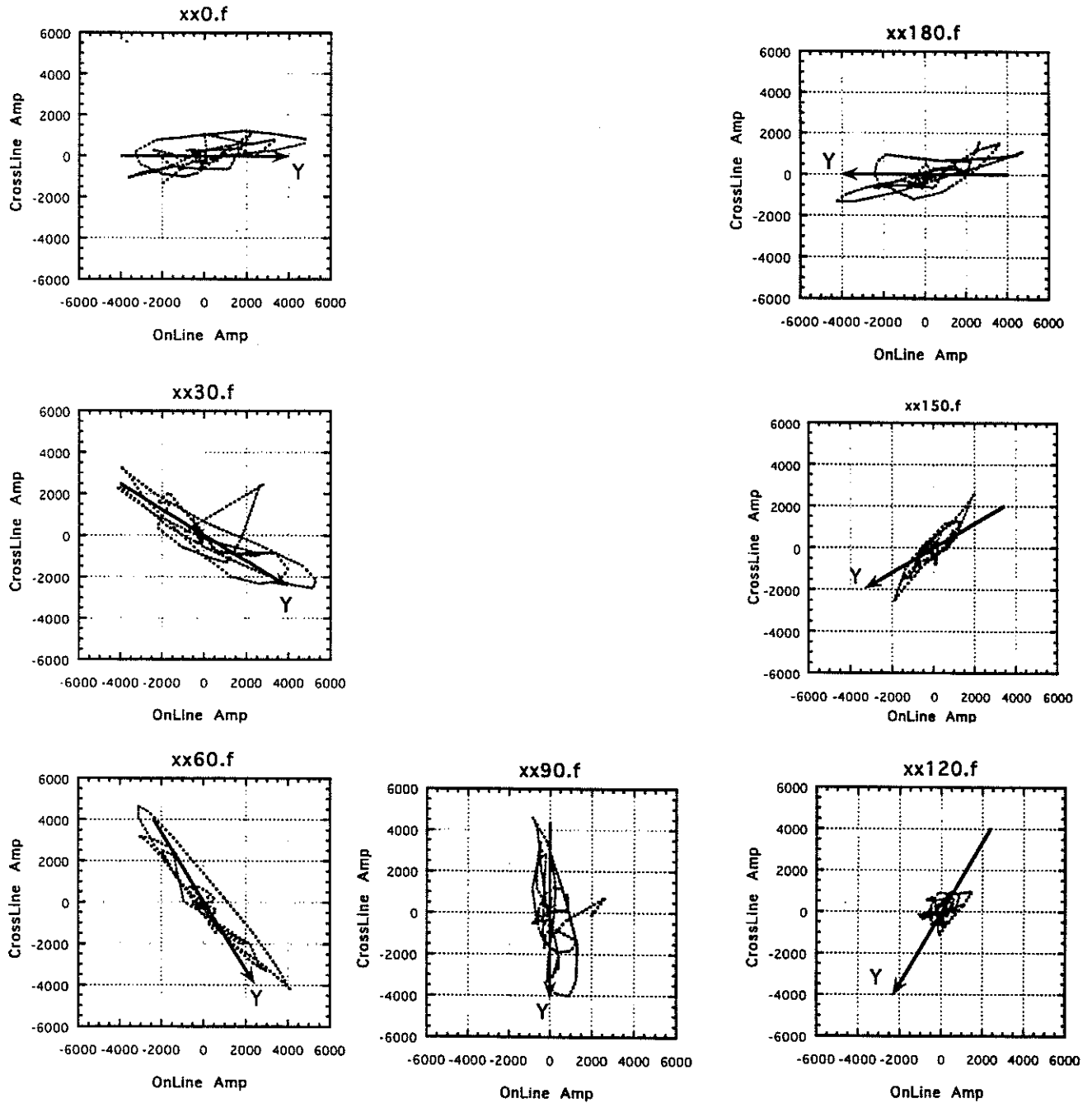


Figure 15: The particle motion of the fast flexural waves received by the dipole receiver in line and cross line in the borehole of phenolite XX-324. The arrow indicates the vibration direction of the fast shear wave.

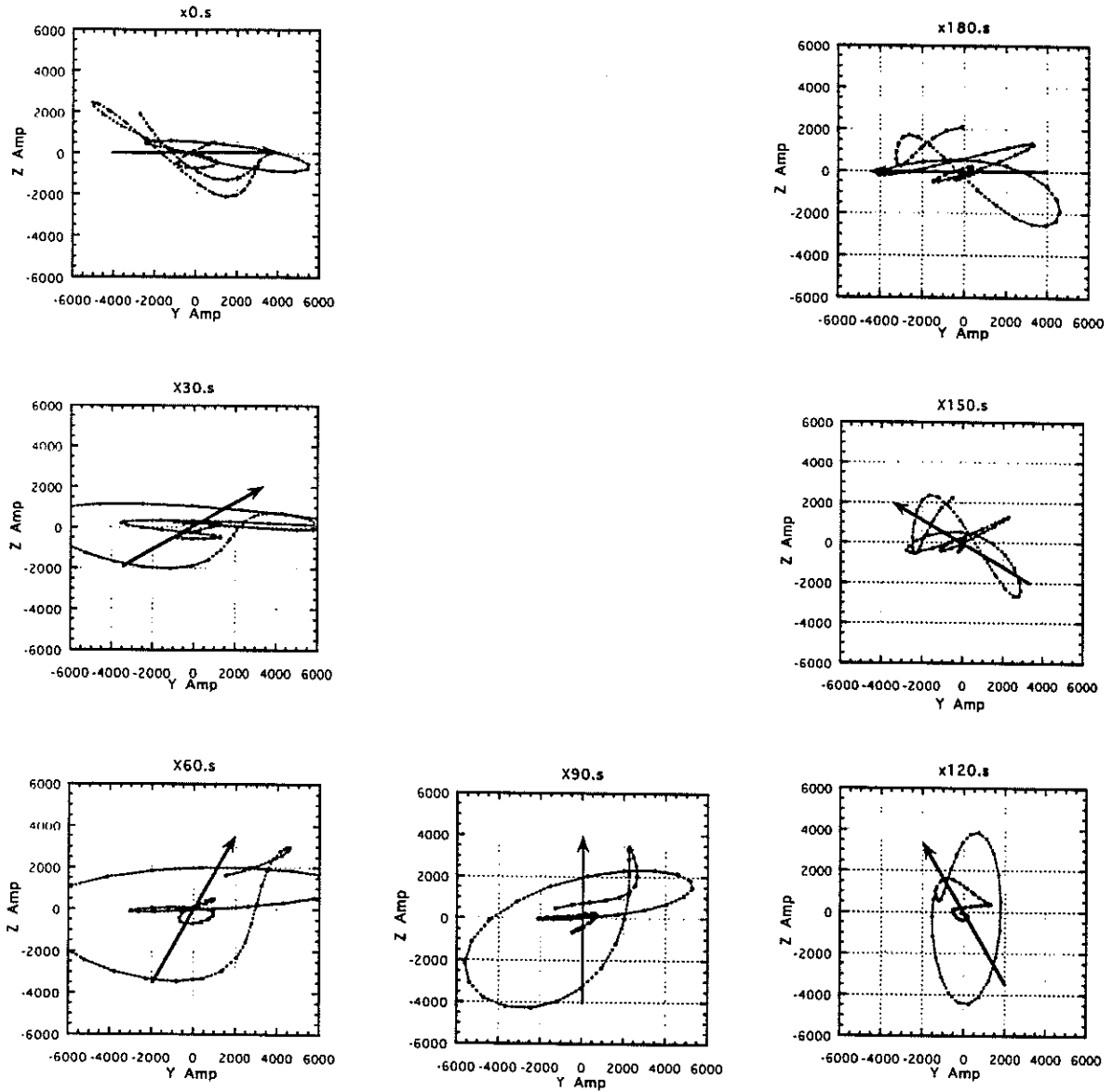


Figure 16: The particle motion of the slow flexural wave in the borehole of the phenolite XX-324. The arrow indicates the direction of the dipole source which is located at  $0^\circ$ ,  $30^\circ$ ,  $60^\circ$ ,  $90^\circ$ ,  $120^\circ$ ,  $150^\circ$ , and  $180^\circ$ , respectively.

## Flexural Waves in an Anisotropic Borehole Model

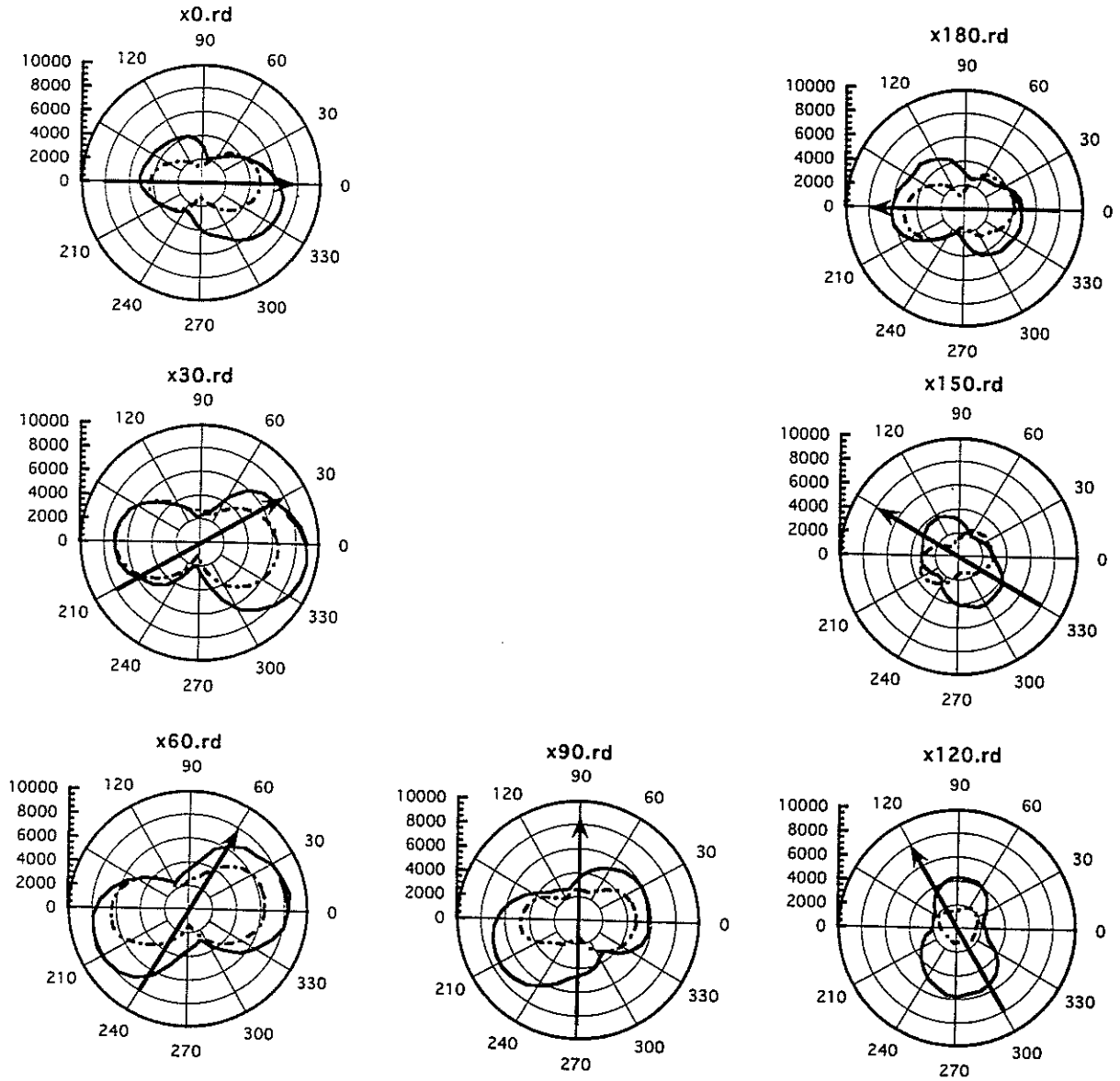


Figure 17: The polarizations of the fast flexural wave (dash line) and slow flexural wave (solid line) in the borehole of phenolite XX-324. The dipole source is located at  $0^\circ$ ,  $30^\circ$ ,  $60^\circ$ ,  $90^\circ$ ,  $120^\circ$ ,  $150^\circ$ , and  $180^\circ$ , respectively. The arrow indicates the direction of the dipole source.

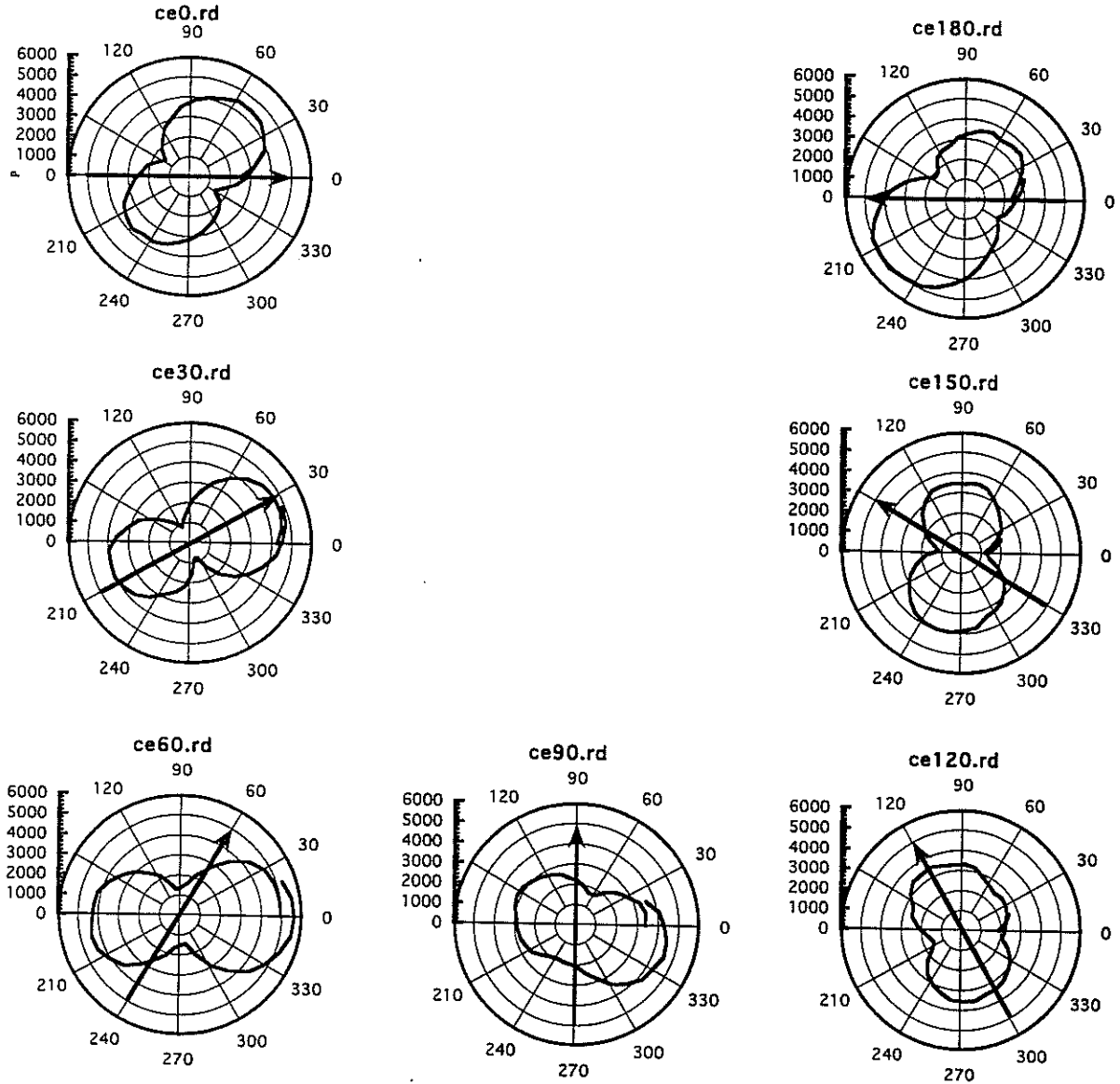


Figure 18: The polarizations of the slow flexural wave in the borehole at X-axis of phenolite CE-578. The dipole source is located at  $0^\circ$ ,  $30^\circ$ ,  $60^\circ$ ,  $90^\circ$ ,  $120^\circ$ ,  $150^\circ$ , and  $180^\circ$ , respectively. The arrow indicates the direction of the dipole source.

## Flexural Waves in an Anisotropic Borehole Model

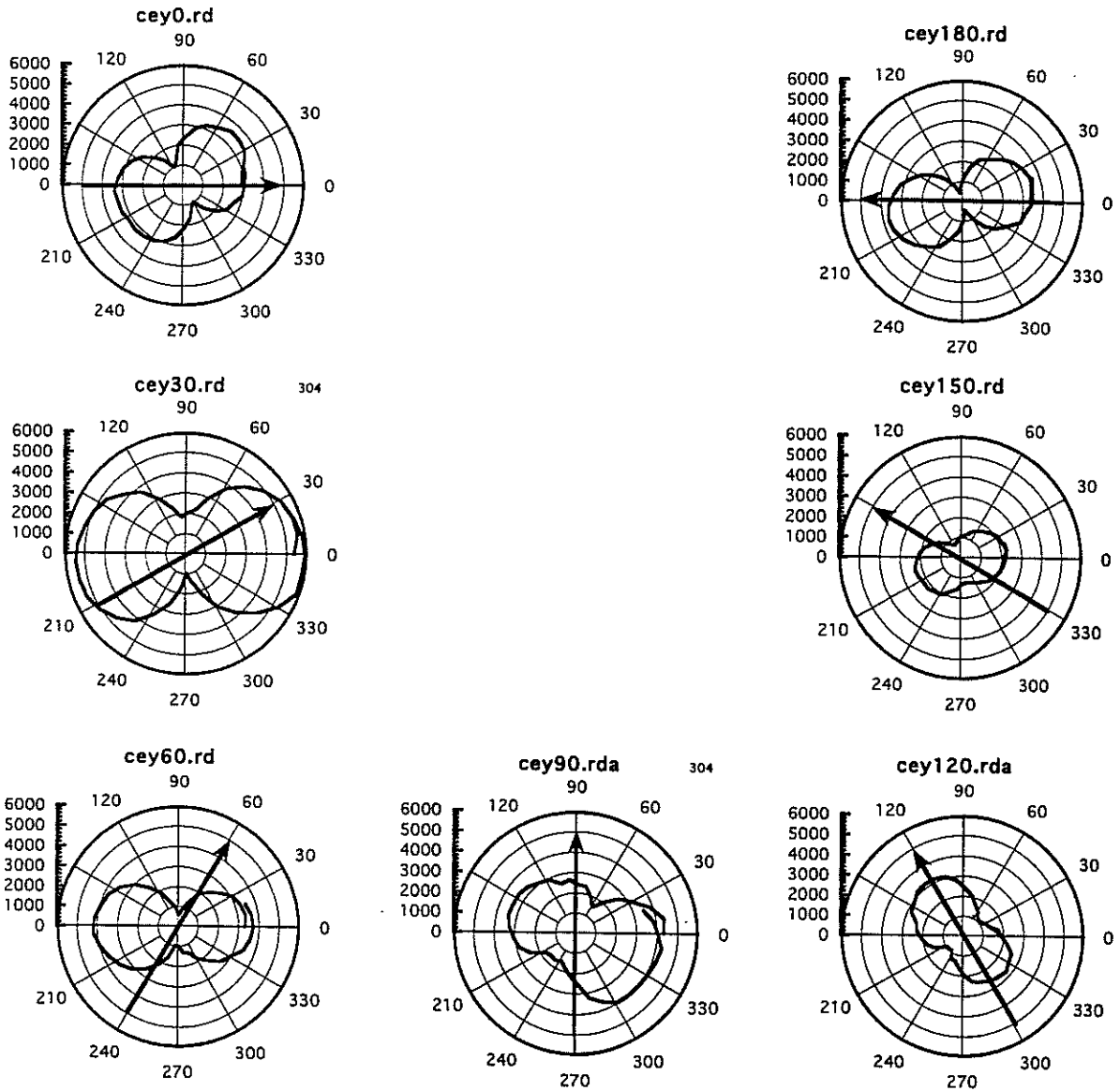


Figure 19: The polarizations of the slow flexural wave in the borehole at Y-axis of phenolite CE-578. The dipole source is located at  $0^\circ$ ,  $30^\circ$ ,  $60^\circ$ ,  $90^\circ$ ,  $120^\circ$ ,  $150^\circ$ , and  $180^\circ$ , respectively. The arrow indicates the direction of the dipole source.

Zhu et al.